Applications of Experimentation on Moseley's Law and X-ray Emission in Undergraduate Instruction

Antoni Bandachowicz

(Dated: March 2022)

We propose two experiments which can be used to instruct undergraduate students on the processes by which X-rays interact with matter. In the first experiment, we analyzed the emission spectrum of a Cu-29 sample by bombarding the sample with electrons, and separating the emitted X-rays using Bragg scattering. We found that K_α emission occurred at an energy of 8240±30 eV and K_β occurred at an energy of 8700±200 eV. This was compared to expected values of 8027 eV and 8902 eV, respectively. The high energy cut-off was also analyzed, and Planck's constant was found to be $6.6\pm0.8\times10^{-34}$ Js, compared to a predicted value of 6.3×10^{-34} Js. By performing this experiment, students learn how to interpret an emission spectrum and how to distinguish between K_α and K_β emission. Our second experiment analyzed the expected linear relationship between K_α values for elements and their $(Z\text{-}1)^2$ values, as predicted by Moseley's law. This experiment was performed using an X-ray beam created from emission due to a Cu-29 sample. The X-ray beam was incident of six different samples of elements. The observed value for the Rydberg constant in this experiment was $1.27\pm0.03\times10^7$ m^{-1}, compared to a predicted value of 1.09×10^7 m^{-1}. In performing this experiment, students learn the importance of calibration, how to interpret goodness-of-fit, and Moseley's law.

I. INTRODUCTION

Data analysis and hypothesis testing are foundational elements of a scientific researcher's abilities. Students should have the opportunity to analyze scientific data and develop their intuition of areas such as atomic physics through experimentation. We suggest that an optimal candidate for this educational requirement is the study of X-rays, due to their uses in material structure and atomic process analysis. X-rays also have many applications in fields such as medicine and astrophysics, from X-ray radiography to satellite imaging [1]. Therefore, the two experiments discussed below obtain information about X-ray emission and Moseley's law, which helps students analyze the energy separation between electron levels of atoms.

In the first experiment, we obtained K_α and K_β emission energies, and the high energy cut-off of Cu-29 with the help of Bragg scattering. K_α emission occurs when an electron within an atom transitions into the innermost K electron shell (with principal quantum number n=1) from a p-orbital of the second shell (denoted with the letter L, and having n=2). K_β emission occurs when an electron transitions into the K electron shell from the $3p$-orbital of the third shell (denoted by M, and having n=3). Together, K_α and K_β energies allow us to characterize the energy values of electron shells of a given atom. Additionally, the high-energy cut-off allows us to determine the energy at which electrons are completely ejected from their respective atoms. These three values allows us to adequately characterize an X-ray emission spectrum. In order to compare the result of the high energy cut-off, Planck's constant is found and compared to currently accepted values.

In second experiment, we confirm the linear relationship between an element's K_α energy, and its $(Z\text{-}1)^2$ value, where Z is the atomic number. This allows us to calculate the expected K_α energy for any atom, and thus the energy difference of its n=2 and n=1 electron shells. Through this experiments, students learn the importance of calibrating equipment readings to understandable values, as well as the importance of goodness-of-fit and comparing data to theoretical relationships.

II. THEORETICAL BACKGROUND

A. Electron Absorption and X-ray Emission

Suppose an electron with charge e=1.60×10^{-19} C is accelerated through a potential difference V within an electron gun and exits with kinetic energy eV. It is directed towards a nucleus of an atom. Depending on the energy of the incident electron, two different processes might occur. The electron can experience deceleration due to coulomb interactions with the nucleus. This deceleration translates in a decrease in the electron's kinetic energy and the emission of a photon, known as "braking radiation". This photon can have any energy within a continuous range from 0 eV to $E_{max} = eV - \Phi$, where Φ is the binding energy of the metal being bombarded, meaning the minimum energy required to remove an electron from the metal in question. Since the experiment uses electrons with kinetic energy in the range of 20 keV, the kinetic energy of the electrons is much larger than the binding energies of Cu-29, and thus the binding energy can be reasonably ignored. As such, we expect the high

energy cut-off to occur at the highest possible energy of the incident electrons, meaning

$$E = eV = \frac{hc}{\lambda} \tag{1}$$

where h is Planck's constant, c is the speed of light, and λ is the wavelength of the emitted X-ray. [2] The incident electron can also eject an electron within the inner shells of the targeted atom. When this happens, the atom becomes unstable, and an electron in a higher energy level will lose energy discretely in the form of an X-ray in order to fill the empty inner shell. The discrete nature of this X-ray emission leads to K_α and K_β lines, which in the first experiment appear as peaks on a graph of emission energy over intensity. As mentioned in section I, In Cu-29, K_α emission occurs when an electron in the n=2 electron shell loses energy to drop into the n=1 electron shell. K_β emission occurs when an electron in the n=2 shell loses energy to transition into the n=1 electron shell [3].

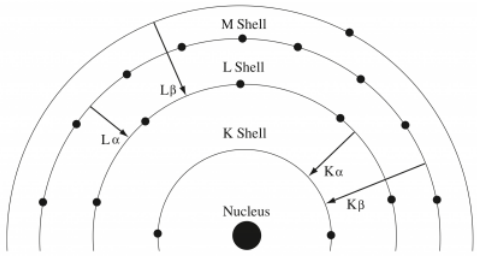

Figure 1: Sketch of K_α and K_β emission of an atom. Notice the different higher energy shells from which electrons transition to fill holes in the K shell due to electron ejection[2].

B. Bragg Scattering

In order to resolve a beam of X-rays , a LiF crystal is used in the Cu-29 emission experiment to make use of Bragg scattering. X-rays incident on the crystal experience Bragg reflection and follow the equation

$$n\lambda = 2dsin\theta \tag{2}$$

where n is the order number (in this experiment n=1), λ is the incident X-ray, d is the distance between atom planes of the crystal, and θ is the angle between the incident ray and the surface of the crystal. Successive layers of atom planes within the crystal form a grating. Thus, in order for refracted phases to add constructively, the angle of incident must equal the angle of diffraction [4]. These two constraints allow us to separate wavelengths into different angles, which in turn will allow us to analyze the intensity of X-rays incident on the detector for a given energy. θ is related to a diffracted X-ray's energy in the following manner

$$E = eV = \frac{hc}{\lambda} = \frac{hc}{2dsin\theta}. \tag{3}$$

C. Moseley's Law

Henry Moseley discovered that a linear relationship exists between the energy of x-rays emitted by an elemental target and the element's atomic number. Moseley's law is derived intuitively from the Bohr model of the atom, where the emitted X-ray energy from an atom is assumed to be equal to the difference between two distinct energy levels. Moseley's law states

$$E = E_i – E_f = 0.75hcR(Z-1)^2 \tag{4}$$

where E is the energy of the K_α line (or the energy at which K_α emission occurs), E_i and E_f are initial and final energies of a transitioning electron, h is Planck's constant, c is the speed of light, R is the Rydberg constant and Z is the atomic number of the element emitting the K_α line [5]. This relationship was used to classify the elements within the framework of the periodic table in the early 20th century [5]. With this law, we can predict the K line emission energy of any known element.

III. EXPERIMENTAL SETUP

A. Cu-29 Emission Spectrum Experiment

When trying the determine the K_α and K_β peaks of the Cu-29 emission spectrum, as well as the high-energy cut-off, the apparatus was setup in the manner illustrated in Figure 1. As seen, X-rays were created in the X-ray tube by bombarding electrons with a known kinetic energy of around 20 keV. These were then collimated by the collimating slit, and the resulting X-ray beam was directed onto the LiF crystal. This crystal in turn used Bragg scattering to diffract the X-rays depending on the incident energies. A carriage arm was able to rotate with a known number of degrees around the crystal, holding a 3 mm and 1 mm slit to help with diffraction grating and shielding of the counter. The counter is located on the carriage arm behind the slits. The counter is connected to a power supply, and dumps its output to the pulse height analyzer (PHA), which was manipulated using UCS-30 software.

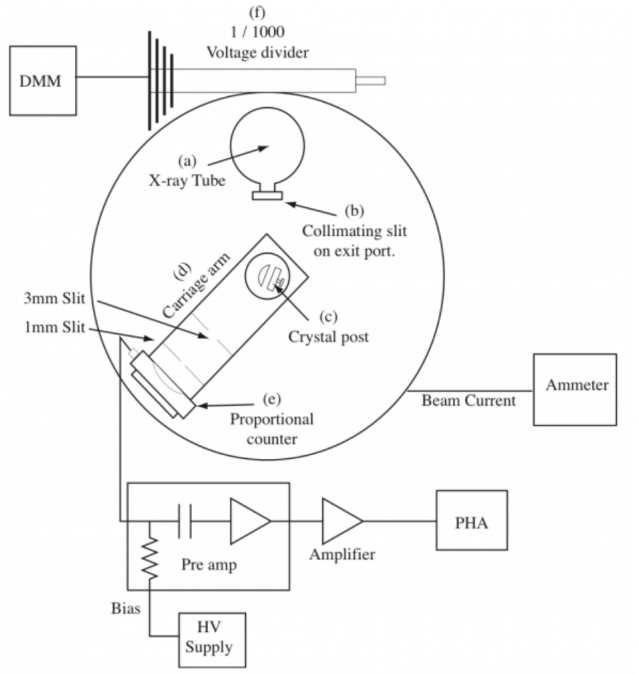

Figure 2: A sketch of the apparatus used for all three experiments. As mentioned, the X-ray tube (a) contains a Cu-29 sample, which cannot be removed. The carriage arm (d) can be rotated 180° around crystal post (c) [2].

B. Moseley's Law Experiment

When determining Moseley's law, the crystal was replaced successively with six different metal samples. The carriage arm was kept in place at a 90° angle with the X-ray beam from the X-ray tube, and both slits were removed.

IV. PROCEDURES

A. Procedure For The Cu-29 Emission Experiment

In order to determine the intensity of emitted X-rays over energy, the carriage arm was moved over a range of angles. Due to time constraints, the entire 180° range of the carriage arm was not mapped. The measurement time for each angle varied, due to differences in intensities. Students should consider why it would be optimal to vary the recording time for different angles. Angles with an associated high intensity had low measurement time, and consequently low uncertainty in intensity, while angles with low intensity had high measurement time and high uncertainty. To standardize results, the intensity for a given angle (and therefore energy) was given by the count rate, meaning count rate = counts / time. For our experiment, we picked angle ranges where the difference in count rate between angles was greatest. This would translate into more data points around the emission peaks. High energy cut-off required us taking data for longer periods of time, due to a low count rate.

B. Procedure For Moseley's Law Experiment

The carriage arm was stationary at 90° from the incident X-ray beam. Additionally, the LiF crystal was removed. This meant that throughout the experiment, the entire energy emission spectrum of a metal was incident on the counter. This meant that the output of the PHA initially represented the entire emission spectrum, separated into channels. These channels needed to be calibrated to emission energy. We found that the relationship between channel number and the emission energy was linear.

After the calibration was performed, the emission spectrum of six different elements was found. Since the entire emission spectrum was gathered and Bragg scattering was not used, we were not able to distinguish between K_α and K_β peaks. We assumed that the highest peak in the spectrum is the K_α peak.

Concerning the X-ray tube and detector specifications, for Cu-29 emission, an accelerating voltage of 20 kV was used for the electron gun and a current of 10 μA was used for the detector. For experimentation with Moseley's law an accelerating voltage of 30 kV was used, with a current of 10 μA.

C. Channel Count to Energy Calibration for Moseley's Law experiment

In order to find the Rydberg constant and graph the relationship between emission energy and atomic number Z, we needed to find the relationship between channel number and energy (in eV). For this procedure, the counts per channel of two metals (Zinc and Vanadium) were fitted using a Gaussian function over the channel number. The peaks found in these Gaussian fits were then plotted with literature energy values, and the relationship between energy and channel number was found using a linear fit (assuming a linear relationship). The Gaussian fits have acceptably large reduced-chi squared values of 4.29 for Vanadium and 2.52 for Zinc.

Metal	Peak Location (Channel)	Energy (eV)
Vanadium	175.5±0.1	3313.9
Zinc	310.0±0.1	8638.9

Table I: Metals used for Moseley's Law experiment calibration. Two Gaussian fits were performed to find peak locations and a linear fit between these two points allowed us to find the relationship between energy and channel number.

V. ANALYSIS

A. Cu-29 X-ray Emission Spectrum

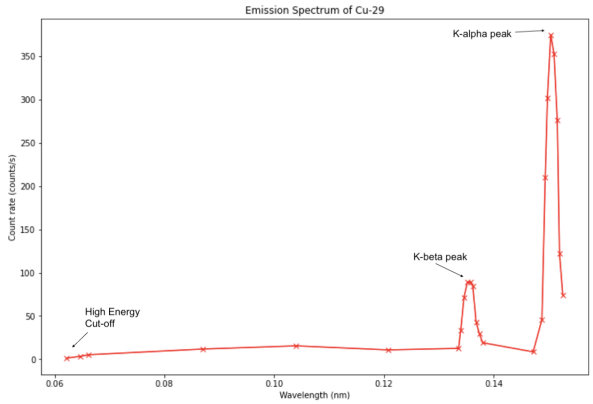

Figure 3: Graph of count rate over wavelength (nm), with identification of emission spectrum features.

Emission Type	Observed Emission Energy (eV)	Expected (eV)
K_α	8200±30	8027
K_β	8700±200	8902

Table II: Observed K_α and K_β values retrieved from Gaussian fits, with uncertainties and predicted values.

The emission spectrum of Cu-29 is depicted in Figure 3, with X-ray wavelength graphed over intensity (count/s). As seen in the theoretical background section, Equation 1 can be used to calculate the corresponding energy of X-rays for a given wavelength. K_α and K_β energy values were determined by fitting the peaks with Gaussian functions, which can be reasonably assumed due to random voltage fluctuations in the detector, among other random influencer variables. The average values gave the central wavelength of the peaks, which could be inputted into Equation 1 to give the corresponding energies.

Students performing this experiment should learn how to distinguish between the two peaks within an emission spectrum. Since K_β occurs due to an electron transitioning from the n=3 energy level to the n=1 level, the resulting emitted X-ray will have a greater energy than an X-ray emitted by K_α emission. This means that the K_β peak will occur at a higher energy than K_α, or equivalently, at a lower wavelength, as seen in Figure 3. Additionally, K_α is more likely to occur than K_β emission, since an n=2 electron is more likely to fill vacancy within the K shell than an n=3 electron. This translates as a higher intensity peak for K_α emission, relative to K_β emission.

Students should also use this experiment to interpret their goodness-of-fit. The fitted peaks had relatively large reduced chi-squared values of 79.30 for the K_α peak and 18.12 for the K_β peak, suggesting that our uncertainties were underestimated. A probable contributor to uncertainty underestimation was the difficulty of setting the equipment to the correct angle, especially at the interval of 1/6th of a degree. The slider would sometimes move on its own by 1/6th of a degree, which would correspond to an uncertainty much larger than the assumed 0.08 degrees.

From Table II we see that K_α emission occurred at 8240±30 eV and K_β emission occurred at 8700±200 eV. The predicted values were 8027 eV and 8902 eV respectively. Neither of the expected values fall within the uncertainty of the observed values. The proximity of the uncertainties to expected value suggest that one reason for the discrepancy might be misalignment of the LiF crystal, which leads to slightly misaligned angles θ and lowers/increases the supposed peak energies depending on the misalignment. Since the entire energy-intensity graph is not shifted relative to predicted values, the more likely reason for the discrepancy is poor fitting accuracy, or the unpredictable movement of the slider mentioned in the previous paragraph.

B. High Energy Cut-Off and Planck's Constant

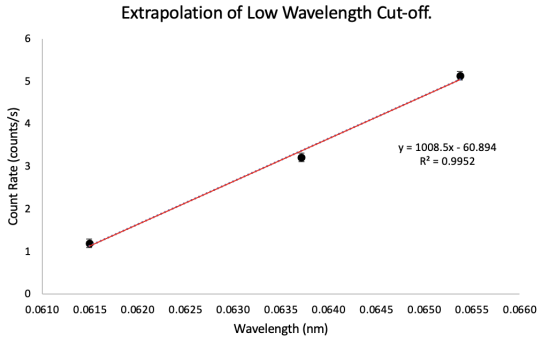

Figure 4: Graph showing linear fit of points near cut-off, with equation used to find the cut-off value.

Extrapolated Cut-off (nm)	Energy cut-off (J)	Observed h (Js)	Expected h (Js)
0.031	$(3.2\pm4)\times10^{-15}$	$(6.6\pm8)\times10^{-34}$	6.26×10^{-34}

Table III: Table showing values of the extrapolated cut-off from the fit in Figure 4, the observed energy cut-off, the observed h, and expected values.

A crucial part of analyzing an emission spectrum is knowing how to identify the high energy cut-off, since it gives researchers information about the binding energy of a given sample. Students should expect this region to be where the count rate for a given angle drops to zero, or near negligible amounts. For calculating the high energy cut-off, a linear fit was performed on wavelengths that yielded the smallest count rates. This linear fit is shown in Figure 4. The extrapolated wavelength gave a value of 0.031±0.004nm. The value was found by using the linear fit equation: Count Rate $= 1939\lambda - 59.22$ and setting it to zero. This leads to an observed h-value of $6.6\pm0.8\times10^{-34}$ Js. Planck's constant was found using the equation $\lambda E/c = h$, where E was the accelerating voltage of 20 kV used to accelerate the incident electrons. The relative uncertainty of h was assumed to be equal to that of λ, since we assume that this was the only variable that contributed a meaningful uncertainty. From this, standard uncertainty in h was found by multiplying the h value by $\frac{\Delta\lambda}{\lambda}$.

From table III, we see that the expected value of h (6.3×10^{-34}Js) is within the uncertainty of the observed value ($6.6\pm0.8\times10^{-34}$Js). However, getting the true value of Planck's constant will prove to be more difficult at more refined intervals, since points leading to the high energy cut-off do not necessarily follow a linear distribution. Additionally, the difficulty in finding Planck's constant will also arise from extremely low count rates near the energy cut-off. Students should be able to appreciate this limitation when reporting their values.

C. Moseley's Law and the Rydberg Constant

Element	Peak Location (Channel number)	$(z-1)^2$	K_α energy (eV)
Nickel	271.1±0.1	729	7099±4
Fe	226.1±0.1	625	5316±4
Cobalt	250.1±0.1	676	6268±4
Cr	191.1±0.2	529	3932±9
Mn	211.0±0.1	576	4719±4
Cu	293.1±0.1	784	7970±2

Table IV: Table showing K_α values for each element, and its appropriate uncertainty, both in eV.

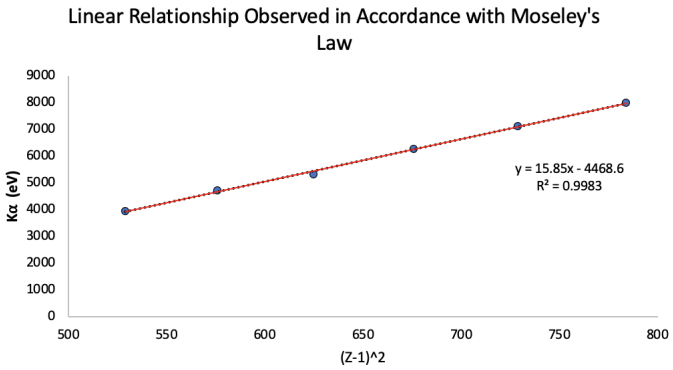

Figure 5: Linear fit of K_α energies over $(Z-1)^2$ values.

Slope (eV)	R (m^{-1})	expexted R (m^{-1})
15.9±0.3	$(1.72\pm0.05)\times10^7$	1.09×10^7

Table V: Observed Rydberg constant with uncertainty and predicted value.

Table IV demonstrates the K_α energy for each of the six elements used. These values were found using the linear fit equation found during calibration:

$$K_\alpha = 39.60x_{cent.} - 3635.7. \tag{5}$$

After the K_α values for each element have been found, the Rydberg constant was found using equation

$$R = \frac{M}{0.75hc} \tag{6}$$

where the slope M of the linear fit in Figure 5 was assumed to be equal to $0.75hcR$. The standard uncertainty of the Rydberg constant was found by using the standard uncertainty in linear fit of the slope and inputting this value into equation 6.

A linear fit was performed, shown in Figure 5, to confirm the relationship dictated by Moseley's law. When analyzing Moseley's law, students should compare the value of constants obtained to their accepted values in order to analyze the accuracy of their results. From Figure 5, the observed Rydberg constant was $1.72\pm0.03\times10^7 m^{-1}$. The expected value is relatively far from the uncertainty range, leading us to conclude that the observed data does not behave according to theory. One reason for this large discrepancy might be due to influences of the copper K_α peak on all the element peaks. Since we are using X-rays produced by bombarding a copper source with electrons, some of the X-rays incident on the metal we are examining might have energy due to copper K_α emission, and might scatter from the element into the detector. This will lead to proportionally more counts around the K_α peak, leading to a shift in the total peak seen in the PHA software. Another reason for the

discrepancy might be an underestimation in the uncertainty due to inaccuracy in the energy calibration, since only two points were used.

VI. CONCLUSION

By performing these two experiments, student gain intuition on how to analyze an emission spectrum, how to perform calibration and goodness-of-fit, and how K_α emission varies from element to element. This is added to the knowledge gained within the areas of radiation and atomic physics.

In the first experiment, we extracted a value of 8240±30 eV for K_α emission, and 8700±200 eV K_β emission. The predicted values were 8027 eV and 8902 eV respectively. High uncertainties in fits were caused by instability of the slider. The high energy cut-off was analyzed, and Planck's constant was found to be $6.6\pm0.8 \times 10^{-34}$J s, compared to a predicted value of 6.3×10^{-34} Js. In the second experiment, the relationship between K_α energies and $(Z-1)^2$ was found to be linear, with a Rydberg constant of $1.72 \pm 0.03 \times 10^7 \mathrm{m}^{-1}$, compared to an expected value of $1.09 \times 10^7 \mathrm{m}^{-1}$.

Overall, we observed data in accordance with theory for Planck's constant h through the emission spectrum. All other observed values had uncertainties that did not encompass predicted values. For all the experiments, a possible misalignment of the LiF crystal might have caused discrepancies with predicted values. Other sources of error included underestimation of uncertainties due to poor function fitting, as well as copper's own emission spectrum, since copper was used for X-ray generation.

As an extension, undergraduate laboratories should consider analyzing the absorption spectrum of an element in conjunction with an emission spectrum, to gain intuition on the difference in energy values between these phenomena, and why this difference occurs. Such an experiment would prove a simple extension, requiring the same apparatus as the one used in our Cu-29 experiment.

VII. APPENDIX

A. Moseley's Law K_α uncertainties

This appendix contains information on how uncertainties for the Moseley's Law experiment were propagated in order to aid students working through similar experiments. The uncertainty in K_α values was found by inputting the standard error of the Gaussian fits SE into Moseley's Law equation. The fit standard error was found through the equation: $SE = \frac{\sigma}{\sqrt{N}}$, where N is the number of counts within the sample used to plot the Gaussian distribution. Thus, the equation for K_α uncertainty is:

$$\Delta K_\alpha = 39.60 \frac{\sigma}{\sqrt{N}}. \tag{7}$$

[1] H. Chen, *Physical Chemistry Chemical Physics*, vol. 39, 2012.

[2] K. V. D. B. Mark Chantell, "X-ray studies," Webpage, 2022.

[3] J. Sinfelt and G. Meitzner, "X-ray absorption edge studies of the electronic structure of metal catalysts," *Accounts of Chemical Research*, vol. 26, 1992.

[4] G. Jauncey, "The scattering of x-rays and bragg's law." *National Academy of Sciences of the United States of America*, pp. 57–60, 1924.

[5] T. Soltis, "One hundred years of moseley's law: An undergraduate experiment with relativistic effects." *American Journal of Physics*, vol. 85, pp. 352–358, 2017.